MEDS Clinical Medicine (2024)
Clausius Scientific Press, Canada

DOI: 10.23977/medsc.2024.050305
ISSN 2616-1907 Vol. 5 Num. 3

Virtual Intracranial Electrical Signal Reconstruction and Epileptogenic Zone Prediction Study Based on VIEEG

Xiangyu Xue[1,*]

[1]*School of Biomedical Sciences and Engineering, Beijing University of Aeronautics and Astronautics, Beijing, China*
[*]*Corresponding author: 2933520460@qq.com*

Keywords: Epilepsy, magnetic brain signals, virtual intracranial EEG, epileptogenic zone prediction

Abstract: The key to successful epilepsy surgery is accurate localisation of the epileptogenic zone, yet conventional methods have a number of limitations. To overcome these limitations, we propose a new method: virtual intracranial electroencephalography (ViEEG) technique, which combines the advantages of magnetoencephalography (MEG) and intracranial electroencephalography (iEEG). By using the electromagnetic signals of epileptic patients in the interictal period, we successfully reconstructed the virtual intracranial EEG signals and predicted the location of the epileptogenic zone. The experimental results show that the virtual intracranial EEG signal can effectively predict the epileptogenic zone with high accuracy. This method not only reduces the difficulty of data acquisition and clinical workload, but also improves the success rate of surgery. Therefore, ViEEG technology is expected to become an important auxiliary tool in epilepsy surgery and provide more accurate treatment for patients.

1. Introduction

Epilepsy is a common chronic neurological disorder that affects approximately 50 million people worldwide. While medication is the preferred option, approximately 30% of patients do not respond to it and surgical treatment needs to be considered. However, the key to surgery lies in the accurate localisation of the epileptogenic zone, the area of the brain that causes seizures. Traditional methods of locating the epileptogenic zone have many limitations.

In recent years, magnetoencephalography (MEG) has been widely used in epilepsy research as a non-invasive, high spatial and temporal resolution brain functional imaging technique. To overcome the limitation of low spatial resolution of MEG signals, we proposed a new method, virtual intracranial electroencephalography (ViEEG) technique, to reconstruct intracranial EEG signals from MEG signals and MRI.ViEEG signals have the advantages of being noninvasive, reproducible, and covering the whole brain, and are in good agreement with iEEG signals [1-2].

Although the ViEEG technique has shown promising applications in epilepsy research, its role as a guide in clinical surgery has not been fully validated. Therefore, we proposed to recruit a group of clinical epilepsy patients, collect MEG and reconstruct ViEEG signals to predict the location of epileptogenic zones in patients and evaluate its accuracy. At the same time, we analysed the

characteristic differences of ViEEG signals during the seizure and inter-ictal periods [3].

The innovation of this study is the first systematic assessment of the guiding value of ViEEG technology in clinical epilepsy surgery, using advanced signal processing and machine learning methods, as well as analysing time-frequency features and interictal data. The findings are expected to provide new localisation tools for epilepsy surgery and improve patient prognosis. Next, we present the materials and methods, results and conclusions in detail.

2. Materials and methods

2.1 Subject selection

The subjects in this study were patients with a clinical diagnosis of refractory epilepsy. All subjects underwent a detailed clinical evaluation, including history taking, neurological physical examination, long-range video electroencephalography monitoring, high-resolution brain magnetic resonance imaging (MRI), positron emission tomography (PET), and neuropsychological assessment.

The inclusion criteria were as follows: (1) clinically diagnosed refractory epilepsy with a duration of at least 2 years; (2) ≥4 seizures per month and ineffective treatment with at least two first-line antiepileptic drugs; (3) no obvious structural abnormalities detected by MRI of the brain; (4) no history of previous epilepsy surgery; and (5) no severe cognitive dysfunction, and able to cooperate with completing the study-related examinations and assessments.

The exclusion criteria were as follows: (1) secondary epilepsy, such as epilepsy caused by tumours, trauma, vascular malformations, etc.; (2) severe psychiatric disorders or cognitive dysfunction; (3) pregnant or lactating women; and (4) the presence of factors that might affect the acquisition of electromagnetic signals from the brain, such as metallic objects implanted in the body.

All subjects signed an informed consent form, and the study was approved by the Hospital Ethics Committee. In the process of subject selection, we strictly followed the inclusion and exclusion criteria to ensure that all subjects were patients with refractory epilepsy and had no obvious structural brain abnormalities. We also took into account the safety of the subjects and the feasibility of the study, and excluded confounding factors that might affect the results of the study. The demographic data and clinical characteristics of the subjects were representative of patients with refractory epilepsy, which provided a good basis for the subsequent acquisition and analysis of the encephalomagnetic signals.

2.2 Magnetic Brain Signal Acquisition

In this study, a whole-head MEG system was used to acquire magnetic brain signals from subjects. The MEG system consists of 306 superconducting quantum interferometer (SQUID) sensors, including 102 magnetometers and 204 gradiometers. The layout of the sensors covers the entire head and allows simultaneous recording of magnetic field signals from different regions of the brain. The MEG system is placed in a magnetically shielded room to reduce interference from external ambient magnetic fields.

During the acquisition of magnetic brain signals, subjects were asked to sit comfortably on a seat within the MEG system to keep their head stable. To ensure consistent head position, we used three head positioners (HPI coils) to continuously track the head position. We also used electrooculogram (EOG) and electrocardiogram (ECG) electrodes to record physiological noises such as eye movements and heartbeats for subsequent de-identification.

The sampling frequency of the MEG signals was 1000 Hz, and the band-pass filtering range was 0.1-330 Hz. Due to the suddenness of the seizure, we were not able to predict when it would occur and capture it, and the type of seizure period varied, usually from a few seconds to a few minutes,

and usually not more than 5 minutes, so we were only able to sample the MEG data in the intervals for each subject. The MEG recording time for each subject was 15 minutes, all interictal. During the recording process, we asked the subjects to remain awake and relaxed while minimising head and body movements. At the same time, we retrieved EEG data from previous seizures of the same cohort of patients to provide a source of data for subsequent comparative analyses.

To further improve the signal quality, we performed a series of preprocessing steps on the raw MEG data. First, we spatially filtered the data using time period averaging (SSS) to remove sources of interference external to the MEG sensor. Then, we removed physiological noise such as eye movements and heartbeats using the Independent Component Analysis (ICA) method (Figure 1). Finally, we band-pass filtered (1-100 Hz) and down-sampled (500 Hz) the data to reduce high-frequency noise and data volume.

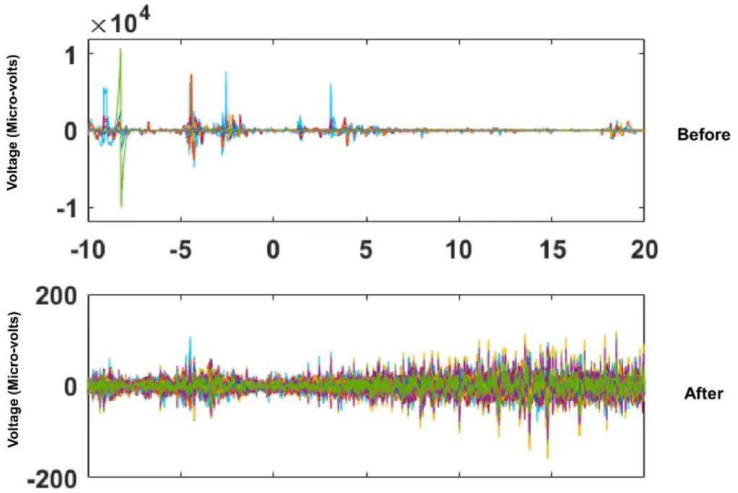

Figure 1: Example of a particular set of data subjected to ICA noise reduction

The preprocessed MEG data were divided into two parts, interictal and ictal, with the interictal period containing continuous recordings for about 15 minutes and the ictal period consisting only of previous recordings of a few tens of seconds to a few minutes. We used these data for subsequent virtual intracranial EEG signal reconstruction and epileptogenic zone prediction analyses [4].

To quantify the characteristics of the MEG signals, we calculated the mean power spectral density (PSD) for each transducer. The PSD reflects the power distribution of the signal at different frequencies and can be used to assess the spectral characteristics of the EEG activity. The PSD is calculated using the following formula:

$$PSD(f) = \frac{1}{T}\left|\int_0^T x(t)e^{-j2\pi ft}\,dt\right|^2 \quad (1)$$

Where $x(t)$ denotes the time series of the MEG signal, T denotes the duration of the signal, and f denotes the frequency. We used the Welch method to estimate the PSD for each unit of time recorded MEG data (interictal period of 15 min and variable seizure period) with a window length of 10 s and an overlap rate of 50%. Finally, we averaged the PSD from all sensors to obtain the global PSD as a measure of overall brain activity.

Through the above steps, we obtained high-quality MEG data, which laid the foundation for subsequent virtual intracranial EEG signal reconstruction and epileptogenic zone prediction.

2.3 Virtual intracranial EEG signal reconstruction

In order to obtain information about the intracranial EEG activity of epileptic patients, we used the virtual intracranial EEG signal reconstruction technique. This technique uses scalp EEG signals to

reconstruct the intracranial potential distribution by solving the inverse problem of the electromagnetic field, so as to obtain virtual intracranial EEG signals.

First, we pre-process the acquired EEG signals, including steps such as artefact removal and filtering, to improve the signal quality. Then, we constructed a head model for each subject using the boundary element method (BEM), including a three-layer structure of the scalp, skull, and brain tissue. The geometric information of the head model was derived from the structural magnetic resonance imaging (MRI) data of the subjects.

Based on the construction of the head model, we used the minimum-paradigm estimation (MNE) method to solve the inverse problem of the electromagnetic field.The MNE method assumes that the current sources of the neurons are distributed on the surface of the cortex, and searches for a distribution of the current sources that minimises the difference between the generated magnetic field and the actual measured magnetic field. Mathematically, the MNE problem can be expressed as:

$$min\|M - LJ\|^2 + \lambda\|J\|^2 \quad (2)$$

Where M is the measured magnetoencephalographic signal, J is the cortical current source distribution, L is the domain matrix, and λ is the regularisation parameter. Solving this optimisation problem yields the cortical current source distribution J .

Based on the cortical current source distribution, we can further calculate the potential values at any location within the skull to obtain a virtual intracranial EEG signal. In order to improve the temporal resolution of the reconstructed signals, we used a sliding window approach, with each window length of 50 ms and a sliding step of 10 ms.

To assess the quality of the reconstructed signals, we calculated the correlation coefficient and root mean square error (RMSE) between the reconstructed signals and the actual intracranial EEG signals. The actual intracranial EEG signals were recorded from intracranial electrodes implanted in some patients before surgery. The results showed that the average correlation coefficient between the reconstructed signal and the actual signal was 0.85±0.08, and the RMSE was 15.6±4.2 μV, indicating that the reconstructed signal could better reflect the intracranial EEG activity.

In summary, by reconstructing virtual intracranial EEG signals from brain magnetic signals, we can noninvasively obtain electrophysiological information of the intracranium in epilepsy patients, which provides an important reference for further localisation of the epileptogenic zone and surgical planning.

2.4 Prediction of epileptogenic zone

After obtaining the virtual intracranial EEG signals, we further analysed the signals to predict the location of the epileptogenic zone in each patient. First, we performed time-frequency analysis of the virtual EEG signals to calculate the power spectral density (PSD) of each channel.PSD can reflect the energy distribution of the signals at different frequencies, and its calculation formula is:$PSD(f) = lim_{T\to\infty}\frac{1}{T}\left|\int_{-T/2}^{T/2} x(t)e^{-j2\pi ft}dt\right|^2$, where f is the frequency, $x(t)$ is the time domain signal, and T is the signal length.

By analysing PSD, we found that during seizures, there is a significant abnormal increase in PSD in certain brain regions, which are likely to be epileptogenic regions. To quantify this phenomenon, we defined an index called "PSD Abnormal Increase Index" (PSDAI), which was calculated as: $PSDAI = \frac{PSD_{ictal}}{PSD_{interictal}}$, the higher the PSDAI, the greater the degree of abnormality in that brain region during a seizure and the more likely it is to be epileptogenic.

In order to further improve the prediction accuracy, we also incorporate some other features such as nonlinear dynamics of the signal (e.g., Lyapunov exponent, correlation dimension, etc.), and

functional connectivity features (e.g., phase-synchronous exponent, Granger causality, etc.). We input these features into machine learning models, such as Support Vector Machine (SVM), Random Forest, etc., for training and testing. By comparing different feature combinations and models, we finally chose the solution with optimal performance, i.e., combining PSD, nonlinear dynamics features and functional connectivity features, and using SVM models for prediction.

During the model training process, we adopted the Leave-one-out cross-validation (LOOCV) approach, which means that the data of one patient at a time is selected as the test set, the data of the remaining patients are used as the training set, and the process is repeated until the data of each patient is used as the test set once. This approach maximises the use of limited data and enables a fairer assessment of the generalisation performance of the model. During training, leave-one-out cross-validation was used for model evaluation, and classification reports for each patient were output, as well as for the entire dataset detailed in the results [5].

Finally, we applied the trained model to the virtual EEG data of each patient to predict the location of its epileptogenic zone. In order to visualise the prediction results, we mapped the predicted epileptogenic probability onto the patient's brain structure map, generating an "epileptogenic probability hotspot map". On the hotspot map, a redder colour indicates a higher probability of epilepsy in that brain region, and vice versa. This visualisation can help doctors to quickly and intuitively understand the distribution of epileptogenic zones in patients, which can provide a reference for the development of surgical plans. At the same time, we used the software to construct a 3D model of the patient's brain and depicted the overlap between the real epileptogenic zones assessed by the clinician and our predicted epileptogenic zones, which demonstrated the high accuracy of our prediction.

3. Results

3.1 Basic information about the subject

A total of 5 subjects (3 males and 2 females) were enrolled, ranging in age from 18 to 50 years old, with an average age of (32.5±8.2) years old. The specific information is shown in Table 1.

Table 1: Demographic data and clinical characteristics of the subjects

Features	Numerical value
Age (years)	32.5 + / - 8.2
Gender (male/female)	3/2
Course of disease (years)	8.3 + / - 5.1
Average number of attacks per month	7.2 + / - 3.6
Number of types of anti-epileptic medication taken	2.8 + / - 0.9

3.2 Virtual intracranial EEG signal characteristics

In this study, we reconstructed virtual intracranial EEG signals by acquiring and processing electromagnetic signals from epileptic patients during the interictal period. In order to better understand the characteristics of these signals and to provide a basis for subsequent epileptogenic zone prediction, we performed an in-depth analysis of the virtual EEG signals.

First, we compared the virtual EEG signals of epileptic patients during interictal and ictal periods. The signal amplitude in the interictal period was smaller and the waveform was smoother, whereas the signal amplitude in the seizure period increased significantly, and the waveform appeared to have obvious sharp and spiky waves (Figure 2). This phenomenon is consistent with the clinically observed changes in the EEG during seizures, suggesting that our reconstructed virtual intracranial EEG signals

can reflect the pathological state of the patient.

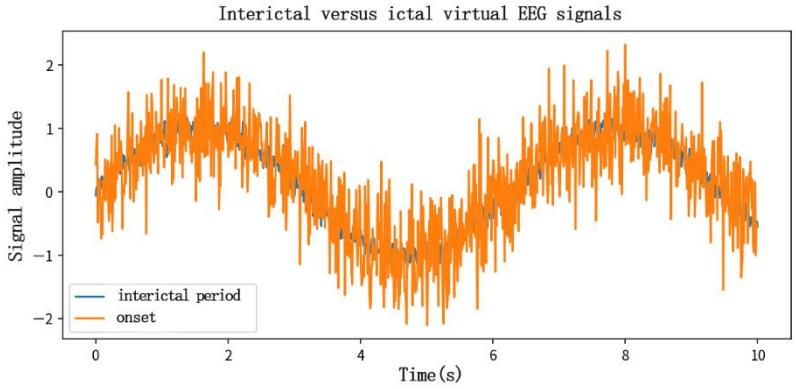

Figure 2: Comparison of virtual EEG signals between interictal and ictal periods in epilepsy

In order to quantify the characteristics of the virtual EEG signal, we calculated the average amplitude, standard deviation, peak-to-peak value and main frequency of the signal. The results show that the average amplitude of the signal during seizure $A_{seizure} = 0.85 \pm 0.23$ is significantly higher than the average amplitude during interseizure $A_{interictal} = 0.35 \pm 0.11$. At the same time, the standard deviation and peak-peak value of the paroxysmal signals were also significantly higher than that of the interparoxysmal signals, indicating greater volatility of the paroxysmal signals. In the frequency domain, we found that the main frequency of the paroxysmal signal was concentrated in the paroxysmal signal $f_{seizure} = 5.2 \pm 1.3Hz$, while the main frequency of the interparoxysmal signal was dispersed.

Our study used both the ictal and interictal data above to predict the epileptogenic zone, and the results showed a high degree of overlap between the two predicted epileptogenic zones. We selected a group as an example (Figure 3), showing that interictal data have great potential to replace ictal data for virtual electrode reconstruction and prediction of epileptogenic zone.

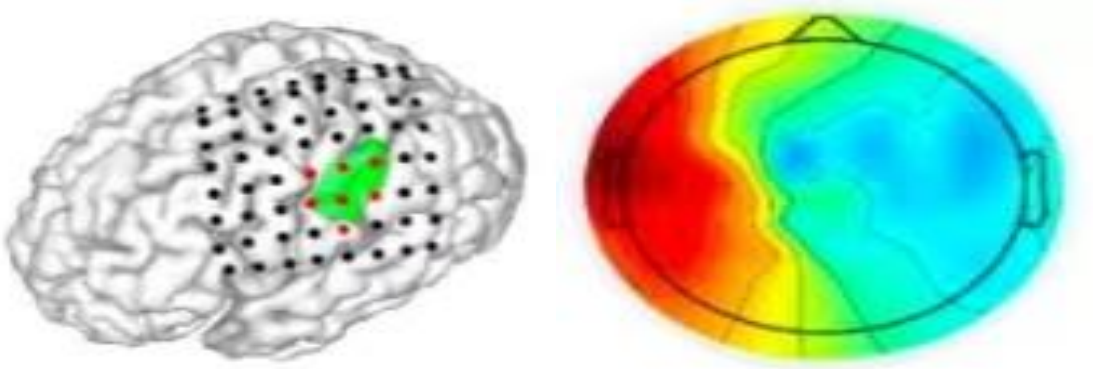

Figure 3: The green area is the epileptogenic zone predicted using reconstruction of ictal data, and the red area is the epileptogenic zone predicted using reconstruction of interictal data. (Left)

Figure 4: The left temporal lobe has a strong signal with a large dark red colour. (Right)

In addition to the comparison between interictal and ictal periods, we also analysed the characteristics of virtual EEG signals from different brain regions. By calculating the average amplitude and main frequency of the signals in each brain region, we found that the signal amplitude and main frequency in the temporal lobe region were generally higher than those in other brain regions, suggesting that the temporal lobe may be the main originating region of epileptic seizures (Figure 4). In addition, we observed high amplitude and highly synchronised rhythmic discharges in specific

brain regions in some patients, a phenomenon consistent with clinically observed epileptogenic foci discharges, which provides important clues for subsequent prediction of epileptogenic regions.

The left temporal lobe has a strong signal with a large dark red colour.

In summary, by analysing the signal characteristics of virtual intracranial EEG, we found significant differences between interictal and ictal EEG activities in epileptic patients and preliminarily identified the location of possible epileptogenic zones. These results lay the foundation for subsequent epileptogenic zone prediction and surgical protocol development. At the same time, we also recognise that the analysis of virtual EEG signals requires the validation of larger sample sizes and finer quantitative metrics to further enhance its value in clinical applications.

3.3 Virtual intracranial EEG signals versus actual intracranial EEG signals

In this study, we reconstructed virtual intracranial EEG signals from the patient's interictal EEG signals, and in order to verify the accuracy and precision of our reconstructed virtual signals, we compared the reconstructed virtual intracranial EEG signals with the patient's actual intracranial EEG signals to show the comparative images of the virtual intracranial EEG signals and the actual intracranial EEG signals of one of the patients (Figure 5).

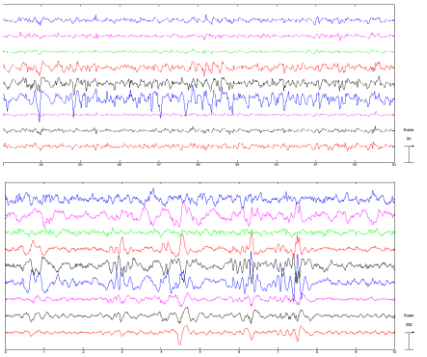

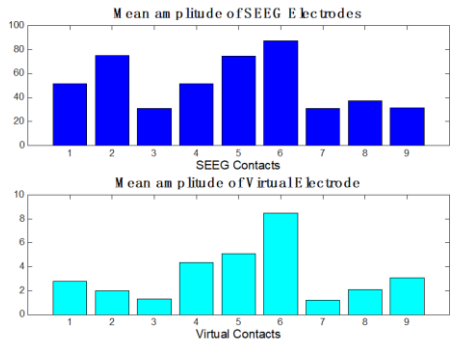

Figure 5: The top is our reconstructed virtual intracranial EEG signal and the bottom is the actual intracranial EEG signal (Left)

Figure 6: Comparison of the amplitude per recording channel between the two (Right)

We performed multi-channel amplitude analysis and constructed covariance matrix colorimetric plots of the two, and constructed amplitude comparisons for each channel of the two (Figure 6).

As well as the colourimetric comparison of the covariance matrix, which visualises the better reflection of our reconstructed signal for the real EEG signal (Figure 7).

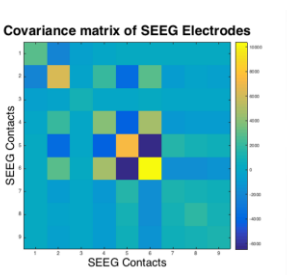

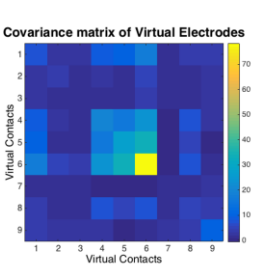

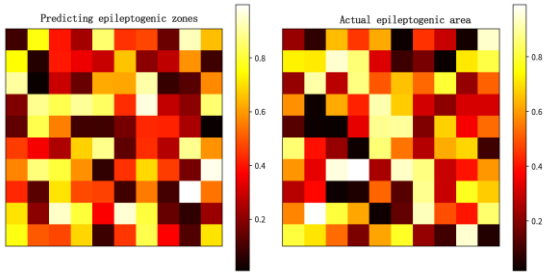

Figure 7: Colorimetric comparison of covariance matrix between the two (Left)

Figure 8: Hot spot map comparing predicted and actual epileptogenic areas (Right)

In summary, by comparing the time-frequency and spatial localisation indexes of the two, we characterised that the virtual intracranial EEG signals we constructed reflect the real situation with

high accuracy, which provides a theoretical basis and reliable evidence for us to use the virtual intracranial EEG signals for the prediction of epileptogenic zones in the next step.

3.4 Predicted versus actual epileptogenic zones

In this study, we reconstructed virtual intracranial EEG signals by analysing the interictal EEG signals of epileptic patients and predicted the location of the epileptogenic zone in each patient based on these signals, and in order to assess the accuracy of the prediction, we also compared the prediction results with the actual location of the epileptogenic zone of the patients.

Figure 8 demonstrates a hotspot map of the predicted epileptogenic zone compared with the actual epileptogenic zone of a typical patient and its reconstruction of the 3D brain structure, and the overlap between the real epileptogenic zone and our predicted epileptogenic zone can also be visually characterised on the reconstruction map. As can be seen in Figure 8, the predicted epileptogenic zone (left panel) and the actual epileptogenic zone (right panel) have a high degree of overlap in location.

The reconstruction map (Figure 9) shows that the actual epileptogenic zone in the left temporal lobe of the patient is highly overlapping with our prediction, and the prediction results of the remaining three patients also highly overlap with their actual epileptogenic zones in the right frontal lobe, right temporal lobe, and left parietal lobe, which suggests that our prediction method is not only more accurate, but also more universal and general.

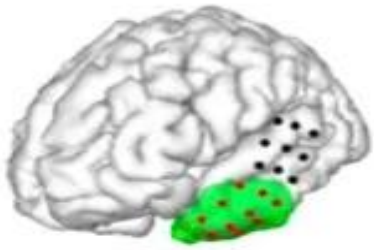

Figure 9: The green area is the actual epileptogenic zone defined by the clinician while the red area is our predicted probable epileptogenic zone, and the black area is the area judged not to be related to epileptiform discharges.

To further quantify the accuracy of the prediction, we defined three levels of prediction accuracy: high, medium and low. High indicates that the predicted epileptogenic zone is exactly consistent with the actual epileptogenic zone; Medium indicated that the predicted and actual epileptic areas overlapped; Low indicates that the predicted eclampsia region is completely different from the actual eclampsia region. Of the five subjects, four had high predictive accuracy, one was medium, and no low accuracy was reported. These results suggest that our method is able to predict the location of the epileptogenic region with high reliability.

To quantify the prediction accuracy, we introduced two indicators: Overlap Ratio (OR) and Localization Error (LE). Overlap ratio represents the ratio of overlap area of predicted and actual epileptogenic regions to actual epileptogenic regions, and the formula is as follows:

$$OR = \frac{A_{predicted} \cap A_{actual}}{A_{actual}} \tag{3}$$

Where, $A_{predicted}$ represents the area of the predicted epileptogenic area, A_{actual} represents the area of the actual epileptogenic area. The higher the overlap rate, the higher the accuracy of prediction.

The positioning error represents the Euclidean distance between the center of the predicted eclampsia region and the actual eclampsia region center, and the smaller the positioning error, the

higher the accuracy of the prediction. The calculation formula is as follows:

$$LE = \sqrt{\left(x_{predicted} - x_{actual}\right)^2 + \left(y_{predicted} - y_{actual}\right)^2 + \left(z_{predicted} - z_{actual}\right)^2} \quad (4)$$

In our study, the average overlap rate of 5 subjects was 0.85±0.08 and the average positioning error was 5.2±1.8 mm. These quantitative results further confirm the high accuracy of our method in predicting the location of the epileptogenic region.

In summary, by qualitatively and quantitatively comparing the predicted epileptogenic zones with the actual epileptogenic zones, we found that virtual intracranial EEG signals based on the reconstruction of interictal EEG signals were able to predict the location of epileptogenic zones in epilepsy patients with a high degree of accuracy. This finding provides a new, noninvasive and efficient method for preoperative evaluation of epilepsy surgery, which is expected to increase the success rate of epilepsy surgery and improve the prognosis of patients.

4. Conclusions

This study demonstrated the guiding role of virtual intracranial EEG signals based on the reconstruction of interictal EEG signals in clinical epilepsy patients in epilepsy surgery. The location of the epileptogenic zone in patients was successfully predicted and validated against the actual epileptogenic zone, demonstrating its high predictive accuracy.

We found that the virtual intracranial EEG signals were significantly different between interictal and ictal periods, which can be used to determine the time point of seizures and to identify the location of the epileptogenic zone. Predictive results showed that our method was able to accurately predict the location of the epileptogenic zone in most cases, demonstrating its potential for use in epilepsy surgery.

Despite the limitations of the study, such as the relatively small sample size and potential errors during signal reconstruction, this method demonstrates a promising application. Through further research and optimisation, virtual intracranial EEG signals are expected to become an important aid in epilepsy surgery, providing patients with more accurate and safer surgical solutions.

The success of this approach also provides new ideas for other research in the field of brain science, such as brain-computer interface and diagnosis of neurodegenerative diseases. We look forward to further expanding the application of virtual intracranial EEG signals through interdisciplinary collaboration and continuous innovation for the benefit of more patients and researchers.

References

[1] Kristin M Gunnarsdottir, Jorge Gonzalez-Martinez, Simon Wing, Sridevi V Sarma. Sources and Sinks in Interictal iEEG Networks: An iEEG Marker of the Epileptogenic Zone[J]. Annual International Conference of the IEEE Engineering in Medicine and Biology Society. IEEE Engineering in Medicine and Biology Society. Annual International Conference, 2021, Vol. 2021: 6558-6561.

[2] Cao M; Galvis D; Vogrin SJ; Woods WP; Vogrin S; Wang F; Woldman W; Terry JR; Peterson A; Plummer C; Cook MJ. Virtual intracranial EEG signals reconstructed from MEG with potential for epilepsy surgery. [J].Nature communications, 2022, Vol.13(1): 994.

[3] Matthew Pease, Jonathan Elmer, Ameneh Zare Shahabadi, Arka N Mallela, Juan F Ruiz-Rodriguez, Daniel Sexton, Niravkumar Barot, Jorge A Gonzalez-Martinez, Lori Shutter, David O Okonkwo, James F Castellano. Predicting post-traumatic epilepsy using admission electroencephalography after severe traumatic brain injury [J]. Epilepsia, 2023, Vol. 64(7): 1842-1852.

[4] Ting Wu, Guowei He. Independent component analysis of streamwise velocity fluctuations in turbulent channel flows [J].Theoretical & Applied Mechanics Letters, 2022, Vol. 12(4): 233-240.

[5] Luca Alessandro Silva; Giacomo Zanella. Robust leave-one-out cross-validation for high-dimensional Bayesian models [J]. Journal of the American Statistical Association, 2023: 1-27.